Results: Experimental data on changes in empathy, theory of mind and moral judgment after mild TBI are surprisingly sparse. The exploration of face and speech perception in mild TBI was usually restricted to patients with comorbid psychiatric conditions. Several studies looked at risk behavior and decision making under risk and uncertainty using Iowa Gambling Task (IGT) in patients with TBI of various severity and one study looked at IGT in patients with mild TBI. The investigation of alexithymia after mild TBI relied exclusively on self-questionnaires.
Conclusion: Changes in social information processing after mild TBI might be related to mild TBI-causally bound pathophysiological mechanisms leading to perturbations in networks for social cognition, pre-injury personality traits, litigation, psychological, emotional and environmental factors. Further research needs to unravel variables that independently predict changes in social information processing domain.

doi:10.1016/j.jns.2015.08.795

726
WFN15-0653
Miscellaneous Topics 3
Modulation of cortical activity in patients with chronic spinal cord injury after intrathecal baclofen

I. Stetkarova[a], R. Jech[b], J. Keller[c]. [a]*Neurology, Third School of Medicine Charles University Hospital Královské Vinohrady, Prague 10, Czech Republic;* [b]*Neurology, 1st Faculty of Medicine and General University Hospital in Prague Czech Republic, Prague 2, Czech Republic;* [c]*Radiology, Na Homolce Hospital Prague Czech Republic, Prague 5, Czech Republic*

Background: Intrathecal baclofen (ITB) is commonly used for severe spasticity due to chronic spinal cord injury (SCI). Clinical effect of ITB on reduction of spasticity is well known; however, mechanism of long-term administration of ITB on the motor system is not fully elucidated.
Objective: To determine which cortical processes are activated during ITB therapy using functional magnetic resonance imaging (fMRI).
Patients and methods: Seven subjects (5 males, aged 20-69 yrs) with chronic SCI (3 with cervical lesions, 4 with thoracic lesions) with no voluntary movement on lower limbs were studied by 1.5 T fMRI with mental movement simulating of foot flexion on the dominant side (one left-handed subject was flipped in x axis). Tasks were performed before and 12 weeks after ITB pump implantation. FMRI data processing was carried out using FEAT (FMRI Expert Analysis Tool) Version 6.00, part of FSL. Second-level analysis was carried out using FLAME stage 1 and 2. Spasticity was assessed by Modified Ashworth scale (MAS). The study obtained Institutional Review Board approval.
Results: ITB treatment profoundly decreased limb spasticity in all subjects (group MAS knee spasticity dropped from 2.7 to 0.44). Second-level analysis ($Z = 2$, cluster significance threshold $p = 0.05$) revealed increase of activation of primary sensorimotor cortex of the foot (Fig. 1).
Conclusions: Continuous ITB administration relieving spasticity in SCI patients was associated with increase of activation of sensorimotor cortex of plegic legs, which may reflect distant functional reorganization of sensorimotor network at cortical level due to positive neuroplastic changes.

Supported by PRVOUK P34, IGA NT12282.

doi:10.1016/j.jns.2015.08.796

727
WFN15-0380
Miscellaneous Topics 3
Factual investigation for solitary patients with subacute myelo-optico-neuropathy in Japan

H. Takada[a], K. Odaira[b], S. Hashimoto[c], M. Konagaya[d]. [a]*Neurology, Aomori National Hospital, Aomori, Japan;* [b]*Regional Medical Liaison Office, Aomori National Hospital, Aomori, Japan;* [c]*Epidemiology, Fujita Health University School of Medicine, Toyoake, Japan;* [d]*Neurology, Suzuka National Hospital, Suzuka, Japan*

Background: Subacute myelo-optico-neuropathy (SMON) is caused by clioquinol intoxication. In Japan, many SMON patients are still afflicted, despite no addition of new patients after 1971. Silvering has been pointed out in medical treatment for SMON patients, and solitary issue is also concerned.
Objective: The aim of this study was to investigate the characteristic features in SMON patients who lived alone.
Patients and methods: We analyzed data from 730 SMON patients that was obtained at medical check-ups carried out by Japanese SMON Research Committee from 2010 to 2012. Neurological and general symptoms classified by severity, activities of daily living (ADL), and care giving condition were surveyed.
Results: Solitary patients tended to increase, from 23.9% in 2010 to 27.8% in 2012. Women occupied over 80%, and the mean age was above 75 years. Regarding the severity of neurological and general symptoms, severely disabled patients were 28% in 2010 and 34% in 2012. For Barthel index, patients whose score was under 60 were 30% in 2010 and 45% in 2012. For ADL, going out was less frequent in solitary patients, and solitary patients tended to feel life dissatisfaction. Twenty-seven percent of patients in solitude did not need care giving, 67% could have care giving when needed, and 5% had no caregiver despite of necessity.
Conclusions: In Japan, not a few number of SMON patients lived by themselves, subsequently for a long period after the exposure to toxicity. Particular application of treatment considered individual care environment should be required for SMON patients who live alone.

doi:10.1016/j.jns.2015.08.797

728
WFN15-0952
Miscellaneous Topics 3
Effects of vitamin B12 and folic acid deficiencies on cogniton: experience from a tertiary center in Turkey

D. Ozyurtlu[a], M.O. Orun[a], A. Sivaci[a], A. Demiralay[a], N. Turkes[a], F.E. Can[b], M. Cavusoglu[a], O. Taskapilioglu[a], H.M. Bakar[a]. [a]*Neurology, Uludag University Medical Faculty, Bursa, Turkey;* [b]*Biostatistics, Uludag University Medical Faculty, Bursa, Turkey*

Vitamin B12 and folate deficiency is an important public health problem in the developing countries. Vitamin B12 and folate deficiency have negative effects on cognitive functions and are associated with increased risk for dementia. This situation not only affects the hematological system but also the neurological system.

The purpose of this study was to investigate the effects of these vitamins on hematological parameters and cognitive performance.

Between 2011-2015, 300 patients admitted to out-patient clinic with forgetfulness were included in the study. Hemoglobin, mean corpusculer volüme (MCV), thrombocyte levels, mini mental state test scores, Beck Depression Scale and Geriatric Depression Scale results of the patients were retrospectively investigated. There was

スモン病患者の認知機能評価

[1]福井大学医学部　神経内科，[2]浙江省人民病院
中嶋　久栄[1]，星野　友佳[1]，遠藤　芳徳[1]，林　　高平[2]，山村　　修[1]，
濱野　忠則[1]

【目的】スモン病はキノホルム（クリオキノール）の過剰摂取により発症した視神経，脊髄，末梢神経を障害する疾患である．クリオキノールは1970年に発売中止となり，それ以降新規の患者はみられていない．しかし近年クリオキノールがアルツハイマー病(AD)をはじめとする認知機能障害に対し有効である可能性を示唆する臨床，基礎研究がみられ，関心を持たれている．今回スモン病検診に参加した5例の認知機能の検討を行った．【方法】スモン病検診に参加した5例（男性3例，女性2例），平均年齢79.8±10.4歳）に対し，MMSE，MoCA-J，ADAS-J Cogを施行した．【結果】MMSEの平均値は26.0±3.3，MoCa-Jの平均値は21.4±4.6，ADAS-J Cogの平均値は8.6±7.0であった．なお，ADAS-J Cogと最も相関が強かった検査はMMSEであった(Spearmanの相関係数-0.986 (P<0.001))．【結論】スモン病患者も高齢化によりADをはじめとする認知症を合併しうる．今回の検討ではクリオキノールが認知機能低下を予防しうるかについては症例数も少なく結論には至らなかった．今後も厳重な経過観察が必要と考えられた．

神経治療　Vol. 32　No. 5（2015）
852

alzheimer's association® | Alzheimer's & Dementia®
THE JOURNAL OF THE ALZHEIMER'S ASSOCIATION

Clioquinol decreases phosphorylation levels of tau protein

Gaoping Lin, Tadanori Hamano, Norimichi Shirafuji, Aiko Ishida, Kouji Hayashi, Shu-Hui Yen, Youshi Fujita, Osamu Yamamura, Yasunari Nakamoto

P2-051

DOI: http://dx.doi.org/10.1016/j.jalz.2015.06.588

Abstract Full Text

Currently, drugs used for Alzheimer's disease (AD) mainly consist of Acetylcholinesterase inhibitors and NMDA receptor antagonist. Those drugs can alleviate AD symptoms, but can't stop or reverse the course of the disease. So researches for drugs that can influence the pathological changes of AD are needed. Bio-metals imbalance may be involved in the formation of senile plaques and neurofibrillary tangles, thus metal modulation may be a direction for treatment of AD. One of metal-protein attenuating compounds (MPACs) clioquinol (CQ) has mild chelating effect for Zn^{2+} and Cu^{2+}.

Medical examination of patients with SMON in Tokushima of 2014

Takao Mitsui , M.D.[#1], Kazuyuki Kawamura , M.D.[#1], Toshio Inui , M.D.[#1], Yutaka Matsuka , M.D.[#2], Maromi Sato , R.N.[#3], Hiromi Hayashi , R.N.[#3], Yuriko Matsuse , R.N.[#3], Kazuhisa Okamoto , P.T.[#4], Miwa Takahashi , Yasunori Saito , [#5], Kaori Morita.[#5], Hiromi Sato .[#5]

#1 . Department of Neurology, Tokushima National Hospital, National Hospital Organization, 1354 Shikiji, Kamojima, Yoshinogawa, Tokushima 776-8585 Japan

#2. Department of Orthopedics, Tokushima National Hospital, National Hospital Organization, 1354 Shikiji, Kamojima, Yoshinogawa, Tokushima 776-8585 Japan

#3 . Department of Nursing department, Tokushima National Hospital, National Hospital Organization, 1354 Shikiji, Kamojima, Yoshinogawa, Tokushima 776-8585 Japan

#4 . Department of Rehabilitation, Tokushima National Hospital, National Hospital Organization, 1354 Shikiji, Kamojima, Yoshinogawa, Tokushima 776-8585 Japan

#5 . Tokushima public health center

Received 25 February 2015; received in received from 27 February 2015; accepted 5 March 2015

Abstract

A medical examination of the SMON in Tokushima of 2014 was reported. There were 28 testees this year. Twenty-seven of them had a medical checkup in a group, seven had a medical checkup at home, and three had a medical checkup in Tokushima National Hospital. This was a similar group of medical examination testees to an average year. There were fore elderly people aged over 90. A medical examination testee decreases gradually with aging of SMON patients. Measures to increase the number of medical examinations by arranging visits are necessary. A future problem may be that many patients are reluctant to be visited at home.

Keywords: SMON in Tokushima, medical checkup, Tokushima National Hospital

Introduction

The sale of chinoform was halted 45 years ago. Subsequently, no new SMON cases were reported. Also, the number of SMON patients decreases with the course. The weathering measures of the SMON are performed as activity such as "gathering workshops of the SMON". We have been checking on the SMON patients in Tokushima every year for many years. In this study, the results for 2014 are reported. Subjects and methods. The subjects were patients with SMON who are resident in Tokushima and enrolled in an SMON investigation individual vote. We conducted a mass checkup and at-home examinations. Furthermore, we checked on the patients hospitalized in Tokushima National Hospital and outpatients of the hospital. We went in the large meeting room of the Tokushima-shi handicapped persons interchange plaza. Three examination areas, each with a medical examination desk and an examination couch were prepared in the meeting room. An electronic height measuring instrument, a set of scales and a sphygmomanometer were

Correspondence to: Takao Mitsui , M.D., Tokushima National Hospital, National Hospital Organization, 1354 Shikiji, Kamojima, Yoshinogawa, Tokushima 776-8585 Japan Phone: +81-883-24-2161 Fax : +81-883-24-8661
e-mail: tmitsui@tokushima-nh.hosp.go.jp

prepared for physical measurement. The physical situation and the present social conditions were described by the SMON patients. Also, a neurological medical examination was conducted.

Results

Thirty people received a medical examination in 2014. They comprised 9 men and 19 women. The average age was 80 years old. The average age at which the disease was contracted was 43 years. The mass checkup covered 22 people. Seven people had a medical examination during an at-home visit. The testees in the Tokushima National Hospital outpatient department numbered two people. The hospitalized patients were alone.

Time of contraction of disease. As shown in Table 1, the age of the patients who had a medical checkup at home was the highest. The age of the patients who had a medical checkup in a group was the second highest. The patients who had outpatient consultations were the youngest. The Barthel Index (78.2 points) of the patients who had a medical checkup at home was the lowest. Most of the patients who received home care had family medicine. Frequent complications included cataract, hypertension, and arthropathy. Many patients were aware of forgetfulness but in four patients this was complicated by obvious dementia. There were fore elderly people older than 90 years. There were two patients with early onset (onset at 18 years old). Two women patients were 65 years old. One had a part-time job; the other was uneasy about single life in the future.

Discussion

Forty-five years have passed since the sale of the chinoform agent was halted in (1970) in 1970 [1]. As a result, it is over 41 years since SMON patients began to contract the disease. The average disease contraction time of SMON patients in Tokushima prefecture is 43 years. The average age of the testees was 78. The number of patients in 1972 when a meeting (patients association) of the Tokushima SMON was organized was 155. The medical examination results that we examined corresponded to the national tendency of the average year. Most patients had family medicine. Even if the patients were living alone, a nearby doctor could be contacted in an emergency. Fore patients were over 90 years old. Three people used nursing care insurance. Furthermore, they received close support from family members. There were two women with young onset (18 years old). The Barthel Index scores for them were 90 and 100 points. The degree of their disorder was very mild. As well as support in terms of food, clothing and shelter, mental support seemed to be needed. The weathering measures of the SMON are performed as activity such as "gathering workshops of the SMON" positively in this study squad. The number of medical examination testees of the aging is shown in (Table 1). A mass checkup in the Tokushima public health center began in 1990. More than forty people participated constantly from 1999. In 2011, the number of the people having an examination decreased. This may be associated with a decrease in the number of testees to have changed a place in a medical examination this year. However, a decrease in the number of testees due to aging will be a main factor. The number of medical examinations conducted at home should be increased.

Reference

1. Konagaya M. SMON: Origin of side-effects of chemical medicine. Iryo. 2009;63:227-234.

Table 1. Patients with SMON that received a medical examination

	Patients			Mean age	Barthel Index
	Men	Women	Total		
Mass checkup	9	13	22	82	82.7
Checkup at home	1	3	4	84	45
Outpatient department	0	2	2	65	95
Hospitalization	0	0	0	-	-

Available online at www.sciencedirect.com
ScienceDirect
www.elsevier.com/locate/brainres
Brain Research

Research Report

Neurotropin promotes NGF signaling through interaction of GM1 ganglioside with Trk neurotrophin receptor in PC12 cells

Yu Fukuda[a,b,d], Takao Fukui[a], Chika Hikichi[a], Tomomasa Ishikawa[a], Kenichiro Murate[a], Takeshi Adachi[d], Hideki Imai[d], Koki Fukuhara[c,d], Akihiro Ueda[a], Allen P. Kaplan[b], Tatsuro Mutoh[a,*]

[a]Department of Neurology, Fujita Health University School of Medicine, Toyoake, Aichi 470-1192, Japan
[b]Division of Pulmonary and Critical Care Medicine, Allergy and Clinical Immunology, Department of Medicine, Medical University of South Carolina, Charleston, SC 29425, USA
[c]The National Institute of Nursing Research, National Institutes of Health, Bethesda, MD 20892, USA
[d]Nippon-Zoki Pharmaceutical Co., Ltd., Osaka 564-0052, Japan

ARTICLE INFO

Article history:
Accepted 20 November 2014
Available online 29 November 2014

Keywords:
Neurotropin
NGF signaling
GM1 ganglioside
Trk tyrosine kinase

ABSTRACT

Activation of the high-affinity nerve growth factor (NGF) receptor Trk occurs through multiple processes consisted of translocation and clustering within the plasma membrane lipid rafts, dimerization and autophosphorylation. Here we found that a nonprotein extract of inflamed rabbit skin inoculated with vaccinia virus (Neurotropin®) enhanced efficiency of NGF signaling. In rat pheochromocytoma PC12 cells overexpressing Trk (PCtrk cells), Neurotropin augmented insufficient neurite outgrowth observed at suboptimal concentration of NGF (2 ng/mL) in a manner depending on Trk kinase activity. Cellular exposure to Neurotropin resulted in an accumulation of Trk-GM1 complexes without affecting dimerization or phosphorylation states of Trk. Following NGF stimulation, Neurotropin significantly facilitated the time course of NGF-induced Trk autophosphorylation. These observations provide a unique mechanism controlling efficiency of NGF signaling, and raise the therapeutic potential of Neurotropin for various neurological conditions associated with neurotrophin dysfunction.

Abbreviations: BDNF, brain-derived neurotrophic factor; BS3, bis(succinimidyl)suberate; cAMP, cyclic AMP; CTB, choleratoxin subunit B; DMEM, Dulbecco's modified Eagle's medium; ECL, enhanced chemiluminescence; ERK, extracellular signal-regulated kinase; GM1, monosialotetrahexosylganglioside; HRP, horseradish peroxidase; NGF, nerve growth factor; PAGE, polyacrylamide gel electrophoresis; PI3K, phosphatidylinositol 3-kinase; PVDF, polyvinylidene fluoride; PY, phosphotyrosine; Tris, tris (hydroxymethyl)aminomethane; Trk, tropomyosin-related kinase

*Corresponding author at: Department of Neurology, Fujita Health University School of Medicine, 1-98 Dengakugakubo, Kustsukake-cho, Toyoake, Aichi 470-1192, Japan. Fax: +81 562 93 1856.
E-mail address: tmutoh@fujita-hu.ac.jp (T. Mutoh).

http://dx.doi.org/10.1016/j.brainres.2014.11.041
0006-8993/

1. Introduction

Nerve growth factor (NGF) stimulates survival and differentiation of sympathetic and sensory neurons (reviewed in Sofroniew et al., 2001). NGF induces morphological and biochemical differentiation of rat pheochromocytoma PC12 cells into a phenotype resembling sympathetic neurons (Greene and Tischler, 1976). NGF initiates its biological actions upon binding to the plasma membrane high-affinity NGF receptor, Trk (Kaplan et al., 1991a; 1991b), which in turn activates intracellular signaling cascades involving pathways depending on extracellular signal-regulated kinase (ERK) and phosphatidylinositol 3-kinase (PI3K) (reviewed in Patapoutian and Reichardt, 2001).

Trk-mediated NGF signaling is initiated by well-coordinated, seamless processes occurred on Trk molecules, which are composed of formation of homodimers (Jing et al., 1992), autophosphorylation of tyrosine residues (Kaplan et al., 1991a) and spatial assemblies with downstream signaling effectors such as Shc and phospholipase C (reviewed in Huang and Reichardt, 2003). Moreover, it has recently become appreciated that molecules requisite for initiating NGF signaling cascade colocalize into certain membrane subdomains, often referred to as lipid rafts, that contain cholesterol and glycosphingolipids (Limpert et al., 2007; reviewed in Hakomori, 2000). While the exact structure and function of neuronal lipid rafts are currently under debate, initiation of NGF signaling is known to be controlled in the lipid rafts by recruitment of signaling molecules and their interactions with lipid components (reviewed in Pike, 2003). As a prime example, it had been shown that monosialoganglioside GM1, a major lipid constituent of the lipid rafts, enhances NGF-dependent homodimerization (Farooqui et al., 1997) and autophosphorylation (Mutoh et al., 1995) of Trk. In addition, GM1 depletion by inhibiting glucosylceramide synthase abolished the NGF response in PC12 cells (Mutoh et al., 1998). These observations clearly indicate structural and functional modulation of Trk by this lipid molecule. Thus, the lipid rafts serve as a highly organized, regulatory core requisite for initiating Trk-mediated NGF signaling.

A non-protein extract of inflamed rabbit skin inoculated with vaccinia virus, designated Neurotropin®, has been widely distributed in Japan and China for the treatment of chronic pain conditions and other various neurologic symptoms. However, precise molecular mechanisms underlying in these pharmacological actions are not fully understood. An active ingredient(s) of this multi-component drug remains yet to be elucidated, in spite of substantial efforts supported by current fractionation technologies such as ultra performance liquid chromatography and capillary electrophoresis. Recently, screening of active ingredients has been started in vitro based on our findings that brain-derived neurotrophic factor (BDNF) expression was augmented in human neuroblastoma SH-SY5Y cells by this drug (Fukuda et al., 2010). Because the BDNF induction by Neurotropin was abolished by co-treatment of the cells with anti-Trk antibody or K252a, a selective inhibitor of Trk tyrosine kinase, it was suggested that targeting and activation of Trk are pivotal for Neurotropin action. In order to test this assumption, here we examined NGF-induced Trk activation in PC12 cells overexpressing Trk (PCtrk cells) (Mutoh et al., 2000). Although Neurotropin itself lacked ability to induce Trk autophosphorylation, it largely facilitated the time course of Trk autophosphorylation in response to NGF. In PCtrk cells exposed to Neurotropin, association of Trk with GM1 ganglioside was found to occur without affecting Trk dimerization and autophosphorylation states. These data implicate that Neurotropin controls the efficiency of Trk-mediated NGF signaling pathway through a novel mechanism associating with ligand-independent interaction of Trk and GM1.

2. Results

2.1. *Trk-dependent promotion of neuritogenesis by Neurotropin*

PC12 cells differentiate into a neuron-like morphology through high-affinity NGF receptor, Trk (Hemstead et al., 1992). In order to evaluate Trk-dependent cellular processes in a steady and sensitive manner, we employed PC12 cells overexpressing human Trk (PCtrk cells) (Mutoh et al., 2000). As expected, NGF (50 ng/mL) dramatically promoted neurite extension, a marker of cellular differentiation, within 24 h (Fig. 1A, Panel c). Neurite extension was not evident at low concentration of NGF (2 ng/mL; Fig. 1A, Panel b), but was enhanced by Neurotropin in a dose-dependent manner (Fig. 1A, Panels d–f; Fig. 1C). Maximal neurite extension was observed at 20 mNU/mL of dosage, and the effect was partly reversed at a higher dosage (100 mNU/mL; Fig. 1C; $P<0.05$ vs. 20 mNU/mL, ANOVA). We also observed a similar biphasic dose-dependency in neurite extension of the parental PC12 cells treated with Neurotropin, confirming that the action was not strain-specific (data not shown). Interestingly, enhancement of neuritogenesis by Neurotropin was not definite in the absence of NGF (Fig. 1B), indicating that Neurotropin may assist the action of NGF in the cells. In addition to such morphological observations, intracellular expression of neurofilament M (NF-M), a major component of the neuronal cytoskeleton supporting axonal construction, was evaluated by Western blot analysis. Expression of NF-M (160 kDa) was significantly augmented by Neurotropin at a dosage of 20 mNU/mL (Fig. 1D). Thus, Neurotropin was shown to enhance neuritogenesis at suboptimal NGF concentration.

We next examined the role for Trk in Neurotropin action by using a selective inhibitor of Trk tyrosine kinase activity, K252a. An enhanced neurite extension by Neurotropin (20 mNU/mL) was drastically prevented by K252a at the concentration effective for inhibition of NGF-induced neuritogenesis (500 nM; Fig. 2A and B). In addition, K252a prevented phosphorylation of intracellular signaling molecules ERK1/2 and Akt induced by NGF or Neurotropin (Fig. 2C). These observations suggest that Neurotropin stimulates neuritogenesis through activations of Trk and downstream signaling molecules.

2.2. *Neurotropin pretreatment facilitates time course of NGF signaling*

In order to characterize the Neurotropin effect on Trk, we next examined the time course of NGF-induced Trk autophosphorylation. Undifferentiated PCtrk cells pretreated for 3 h with

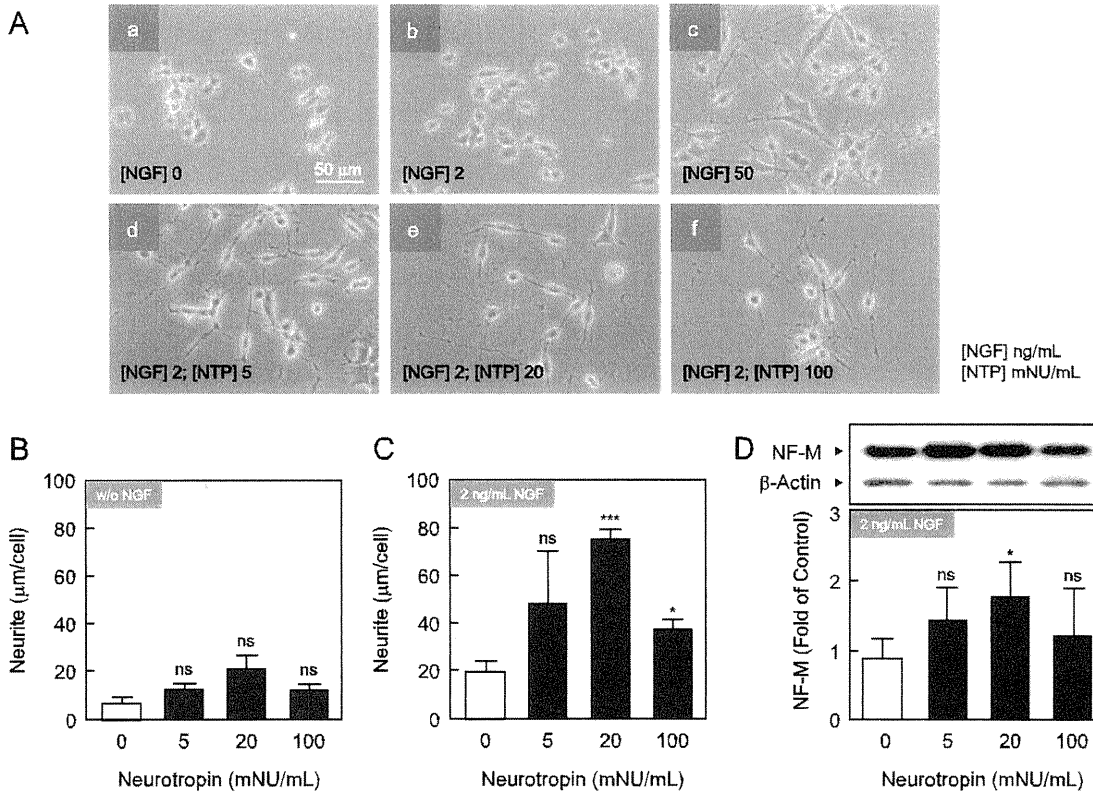

Fig. 1 – Neurotropin promotes neurite outgrowth in PCtrk cells treated at suboptimal concentration of NGF. **(A) Neurite extension by Neurotropin. PCtrk cells (1000 cells per well, 6-well plastic plate) were treated for 24 h in the absence (*a*) or the presence of NGF (*b*, *d–f*, 2 ng; c, 50 ng/mL) and Neurotropin (NTP; *d*, 5 mNU; *e*, 20 mNU; *f*, 100 mNU/mL). Phase-contrast micrographs taken for typical areas of cultures were shown. (Bar = 50 μm in length) (B) and (C). Effect by Neurotropin on neurite length. PCtrk cells were cultured for 24 h in the absence (B) or the presence of NGF (2 ng/mL, C) and indicated concentrations of Neurotropin (0, 5, 20, or 100 mNU/mL). Neurite length was measured by Image J as described in** Section 4. **Data represents the mean and standard deviations (SD) of neurite length in three independent cultures. (D) Neurofilament M (NF-M) expression. Cell lysates of PCtrk cells (1×10^5 cells, 26 h) were subjected to Western blotting against NF-M and β-actin (an internal control) as described in** Section 4 **(*upper panel*, typical blotting images). Data represents the mean and SD of the intensity ratio of NF-M to β-actin in three independent cultures.** $^*P < 0.05$, $^{**}P < 0.001$ **vs. saline-treated controls (*open bars*); ns, not significant (two-sided *t*-test).**

saline (control) or Neurotropin at 20 mNU/mL, an effective concentration for neuritogenesis (see Fig. 1), were incubated with NGF (50 ng/mL) for various time periods (0.5–20 min), and tyrosine phosphorylation of Trk was examined by a double-antibody ELISA using antibodies against Trk (α-Trk) and phosphotyrosine (α–PY) for cell lysates (Fig. 3A), or by Western blot analysis against phosphotyrosine (PY) in α-Trk immunoprecipitates (Fig. 3B). NGF-induced Trk autophosphorylation was observed in a time-dependent fashion, peaking at 5 min (Fig. 3A, open symbols). To our surprise, pre-exposure of PCtrk cells to Neurotropin (20 mNU/mL, 37 °C, 3 h) significantly accelerated the time course of NGF-induced Trk autophosphorylation, although total and peak intensities of phosphorylated Trk were virtually unaffected (Fig. 3A, closed symbols). Since basal levels of phosphorylated Trk without NGF stimulation were equivalent between treatments (Fig. 3A and B, time "0"), Neurotropin seemed not to enhance Trk phosphorylation directly, but rather to improve the efficiency of Trk-mediated NGF signaling.

2.3. *Neurotropin promotes Trk-GM1 association*

We have previously reported that GM1 associates with Trk and enhances NGF signaling in PC12 cells (Mutoh et al., 1995). It is believed that this process involves translocation of Trk molecules into compartmentalized microdomains in the plasma membrane, so-called lipid rafts, where GM1 and other glycosphingolipids reside. Accordingly, we next examined the effect of Neurotropin on the receptor-lipid association. Immunoprecipitates with α-Trk from PCtrk cells incubated with NGF (1 min) and/or Neurotropin (1 min or 3 h) were subjected to SDS-PAGE for Western blot analysis against GM1. Multiple bands were probed by anti-GM1 antibody (α–GM1) as shown in Fig. 4 (Panel C). NGF treatment gave a strongly immunoreactive band approximately at 140 kDa (lane 2, *asterisk*), corresponding to the molecular size of Trk. This observation indicates NGF-dependent formation of the Trk–GM1 complex that is resistant to sample treatment with SDS as previously reported (Mutoh et al., 1995). Both the receptor-lipid association (Panels C and E) and Trk autophosphorylation (Panels A, B and

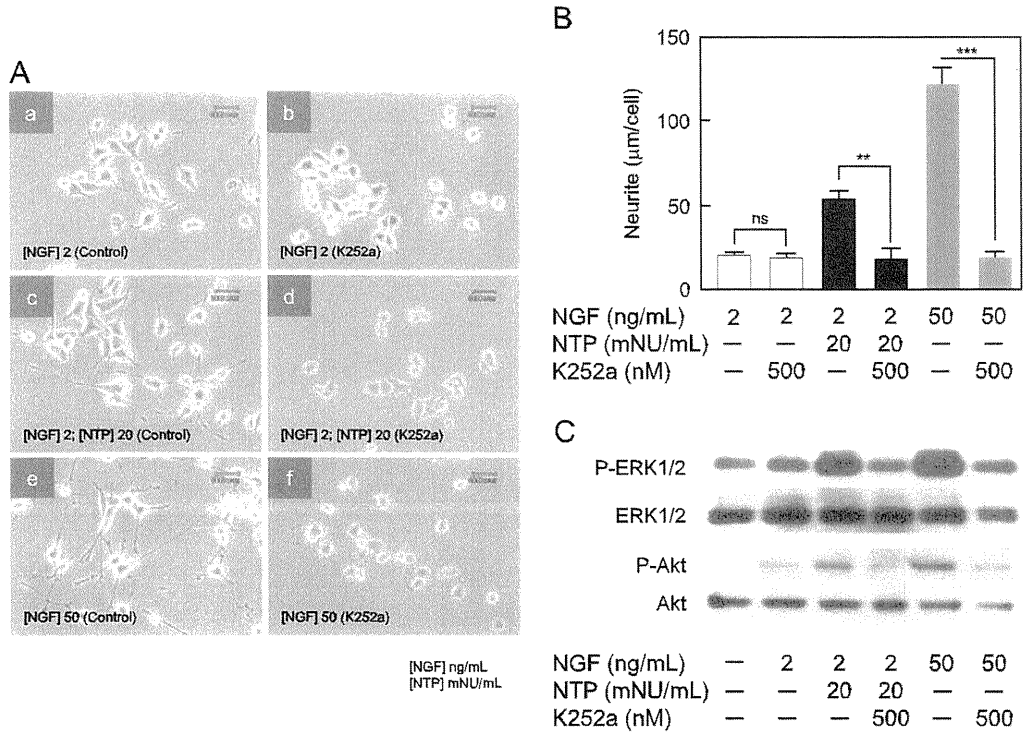

Fig. 2 – Role of Trk in Neurotropin action. (A) Neurite extension by Neurotropin was blocked by K252a. PCtrk cells (1000 cells per well) cultured in serum-free DMEM in the presence of NGF (*a–d*, 2 ng/mL; *e*, *f*, 50 ng/mL) and/or Neurotropin (*c*, *d*, 20 mNU/mL) were treated with K252a (500 nM; *b*, *d*, *f*) for 6 h prior termination of the culture for 18 h. Phase-contrast micrographs were taken for typical areas of cultures. (Bar = 30 μm in length) From three independent cultures, neurite length was quantified by Image J software as described in Section 4. (B) Data represents the mean and SD. ns, not significant; $^{**}P<0.01$, $^{***}P<0.001$ vs. controls in the absence of K252a (*t*-test). (C) Involvement of ERK1/2 and Akt in Neurotropin action. PCtrk cells (1×10^5 cells) were treated for 24 h in serum-free DMEM containing NGF and/or Neurotropin as indicated. K252a (500 nM) was added at 30 min prior termination of the treatment. Cells were lysed in SDS sample buffer, and the lysate was subjected to Western blot analysis detecting phosphorylated and total forms of ERK1/2 (P-ERK1/2 and ERK1/2, respectively, *upper panels*) or Akt (P-Akt and Akt, respectively, *lower panels*) as described in Section 4.

D) by NGF was enhanced by prolonged incubation with Neurotropin in the presence of Neurotropin (Panels A–C, lanes 4 and 6). Intriguingly, even in the absence of NGF, a 3-h exposure to Neurotropin at 20 mNU/mL stimulated association of Trk and GM1, without affecting Trk autophosphorylation (Panels A–C, lane 5). Thus, Neurotropin induced association of Trk and GM1, which may determine response acquisition of the cells to NGF stimulation. In addition, these observations strongly suggest that such receptor–lipid complex can be constructed independently of Trk autophosphorylation.

2.4. *Effect on Trk homodimerization*

Since dimer formation of Trk promotes efficient autophosphorylation by NGF (Jing et al., 1992), we next tested the effect of Neurotropin on the receptor homodimerization (Fig. 5). Cell surface molecules in PCtrk cells treated with NGF (50 ng/mL, 5-min stimulation) or Neurotropin (20 mNU/mL, 3-h exposure) were crosslinked with a membrane impermeable, bifunctional crosslinker BS3, followed by immunoprecipitation of the cell lysates with α-Trk antibody. Western blotting showed that Trk homodimer (approximately 300 kDa in size) was significantly formed by NGF (lane 2; $P=0.043$ vs. untreated control), but not by Neurotropin alone (lane 3; $P>0.05$). These data suggest that formation of the receptor dimer depends on the presence of NGF, but is not stimulated by Neurotropin.

3. Discussion

In this study, neuritogenic action of Neurotropin was found to accompany interaction of Trk and GM1 in PCtrk cells. In NGF signaling, GM1 potentiates Trk responsiveness at least in the steps of homodimerization (Farooqui et al., 1997) and autophosphorylation (Rabin and Mocchetti, 1995) presumably by a direct association with each other to form Trk–GM1 complex (Mutoh et al., 1995). However, little is known about the precise mechanisms of functional modulation of Trk by GM1. In our experiments, since 3-h exposure to Neurotropin stimulated endogenous GM1 association with Trk without affecting dimerization and autophosphorylation (Figs. 4 and 5), the association of endogenous GM1 is confirmed to be an antecedent event which is dissociable from the subsequent dimerization and phosphorylation processes. Oppositely, a brief Neurotropin treatment failed to induce apparent complex formation

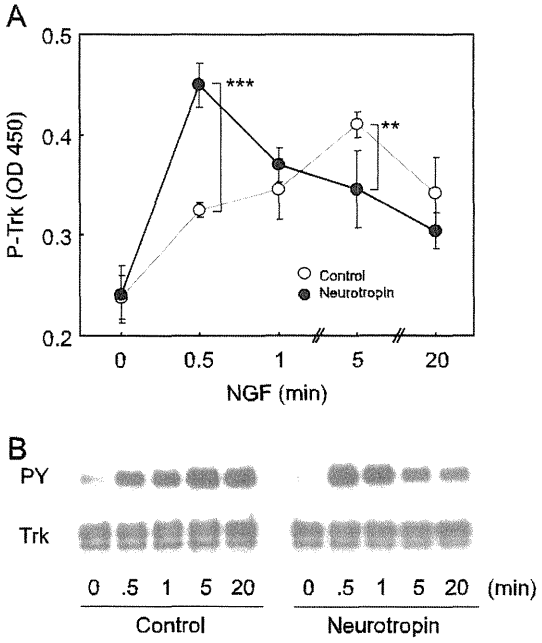

Fig. 3 – Facilitation of NGF signaling by Neurotropin. Serum-free culture of PCtrk cells (5×10^5 cells) was pretreated with 20 mNU/mL of Neurotropin for 3 h, and stimulated with 50 ng/mL of NGF for indicated time period (0, 0.5, 1, 5, or 20 min). The cells were immediately lysed at 4 °C, and the lysate was subjected to ELISA assay (A) and Western blot analysis (B) for determination of Trk autophosphorylation. (A) The cell lysates containing equal amount of proteins were directly assayed by ELISA assisted by α-Trk and α-PY as described in Section 4. Phosphorylated Trk levels (P-Trk) were expressed as OD at 450 nm of the reaction mixture. Data represents the mean and SD of 4 independent experiments. Open circles, saline-treated controls; closed circles, Neurotropin pretreatment (20 mNU/mL, 3 h). Statistically significant induction of Trk phosphorylation was observed after treatment both in control and neurotropin-treated cultures ($P<0.001$ vs. 0 min; Dunnett-type comparison). $^{***}P<0.001$, $^{**}P<0.01$ vs. saline-treated controls (ANOVA). (B) The lysates were immunoprecipitated by α-Trk, and subjected to SDS-5–20% PAGE, followed by Western blot analysis against total (Trk) or phosphorylated (PY) forms of Trk as described in Section 4. Each lane contained equal amount of proteins. Representative images are shown.

between Trk and GM1 (1 min, Fig. 4C, lane 3). A similar time-requiring process was also reported for exogenously supplied GM1 in the induction of Trk autophosphorylation with an interval of 1 h or 6 h (Rabin and Mocchetti, 1995). Neurotropin action may involve such time-consuming events as redistribution and assembly of Trk molecules into GM1-rich environment like lipid rafts, leading an efficient NGF signaling (Limpert et al., 2007). In agreement with this notion, PCtrk cells with prolonged Neurotropin treatment (3 h) showed a significantly accelerated time frame of Trk autophosphorylation response by NGF (Fig. 3). These observations suggest that Neurotropin enabled rapid cellular responses to NGF probably through the formation of Trk–GM1 complexes, although underlying precise mechanism by which Trk–GM1 complexes are formed remains to be elucidated.

In the present study, Neurotropin was demonstrated to induce neurite extension in the presence of suboptimal concentration of NGF (2 ng/mL; Fig. 1). Neuritogenic actions by Neurotropin had been reported for the first time by Morita et al. (1998), where Neurotropin enhanced neurite outgrowth of PC12h cells, a subclone of PC12 cells which also responds to NGF (Hatanaka, 1981), independently of cAMP-driven pathways. Recently, neuroprotective actions of Neurotropin had been demonstrated in PC12 cells and primary dorsal ganglion neurons manifested by neurite degeneration induced by anticancer agents such as paclitaxel (Kawashiri et al., 2009) and oxaliplatin (Kawashiri et al., 2011). In addition, a cytoprotective action of Neurotropin has been reported on oxidant-exposed lung A549 cells by inducing a redox-regulating molecule, thioredoxin-1 (Hoshino et al., 2007). Thioredoxin-1 is recognized as a neurotrophic co-factor having a regulatory role in NGF-mediated signal transduction in PC12 cells (Bai et al., 2003). Furthermore, our recent approaches employing human neuroblastoma SH-SY5Y cells revealed that Neurotropin activates the biosynthesis of brain-derived neurotrophic factor (BDNF) (Fukuda et al., 2010). The effect involved activation of PI3K, ERK and cAMP-responsive element binding protein. Since these intracellular signaling pathways in neurons are known to be initiated by Trk receptors (reviewed in Huang and Reichardt, 2003), these independent observations may share the molecular mechanism as described in this report. Consistently, effective concentrations of Neurotropin needed for all these phenomena observed in vitro were between 10 and 100 mNU/mL.

Association of abnormalities in Trk-mediated intracellular signaling has been implicated in numerous disorders such as Alzheimer's disease, stroke, amytrophic lateral sclerosis (ALS) and diabetic neuropathy (see review by Chao et al., 2006). Mutations in the tyrosine kinase domain of Trk have been reported in patients with congenital insensitivity to pain with anhidrosis (CIPA), an autosomal-recessive disorder characterized by recurrent episodes of unexplained fever, absence of sweating, absence of response to noxious stimuli, self-mutilating behavior and mental retardation (Indo et al., 1996). In addition, we found α-Trk autoantibodies in patients with subacute sensory neuropathy, which provoked a functional disturbance of the Trk-mediated signaling in PCtrk cells (Mutoh et al., 2005). Moreover, we recently documented that clioquinol, a causative agent of subacute myelo-optico neuropathy (SMON), interrupted NGF-induced Trk signaling and neurite outgrowth in PC12 cells (Asakura et al., 2009). These observations suggest the importance of Trk-mediated signaling in the maintenance of the autonomic, peripheral and central nervous systems. Based on clinical experiences over a half century in Japan, Neurotropin had been noted to possess therapeutic potential for various neurological disorders associated with neurotrophin signaling dysfunction, such as ischemic brain infarction (De Reuck et al., 1994), senile dementia (Kimura et al., 1987), SMON-associated dysesthesia (Sobue et al., 1992), and chemotherapy-induced neuropathy (Zhang et al., 2012). Translational studies using corresponding animal models are now conducted to evaluate the contribution of Trk-mediated NGF signaling in clinical effectiveness of Neurotropin.

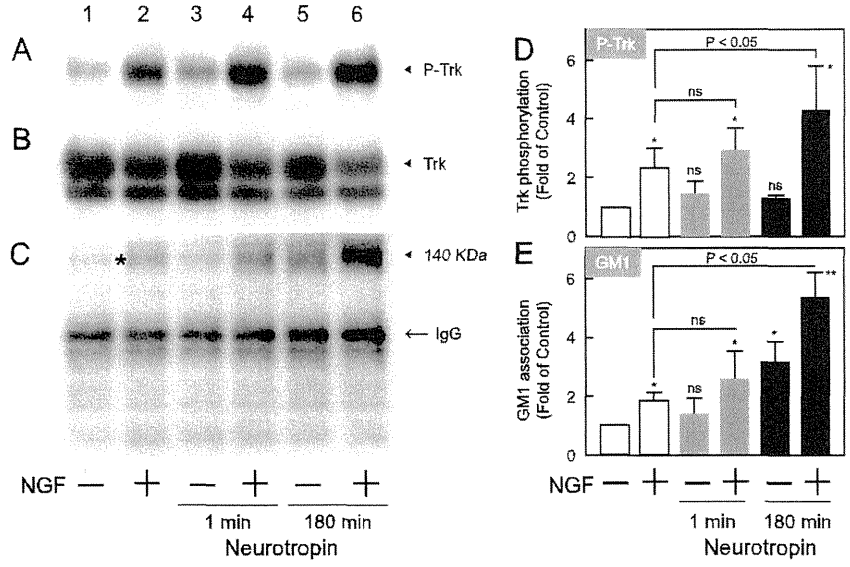

Fig. 4 – NGF-independent association of Trk and GM1 in PCtrk cells treated with Neurotropin. (A–C) Serum-free culture of PCtrk cells (5×10^5 cells) was pretreated with saline (*lanes* 1 to 4) or 20 mNU/mL of Neurotropin (*lanes* 5 *and* 6) for 3 h, and stimulated with 50 ng/mL of NGF for 1 min at 37 °C (*lanes* 2, 4, *and* 6). For *lanes* 3 *and* 4, Neurotropin (20 mNU/mL) was added simultaneously with NGF and treated only for 1 min. Western blot analyses of α-Trk immunoprecipitates against phosphorylated ((A) P-Trk), total ((B) Trk) forms of Trk, or GM1 ganglioside (C) were performed as described in Section 4. Anti-GM1 antibody primary recognized a broad band around 140 kDa (corresponding to the size of Trk), whereas secondary antibody recognized α-Trk IgGs used for immunoprecipitation (*arrow*, ca. 50 kDa). When focused on the 140-kDa band, Neurotropin alone stimulated an association of GM1 immunoreactivity in α-Trk immunoprecipitates even in the absence of NGF ((C), *lane* 5). The mean and SD of activated Trk ((D) PY in panel A) and Trk-associated GM1 ((E) a 140-kDa band in panel C) were summarized by three independent experiments. Data was represented as fold induction of saline-treated control (1.0). *$P < 0.05$; **$P < 0.01$ vs. saline-treated controls without NGF stimulation; ns, not significant (Student *t*-test).

Neurotrophins have potential for the treatment of neurological diseases. However, their therapeutic application has been largely limited because of their poor pharmacological properties, such as low stability in serum, restricted penetration across blood–brain barrier, minimal diffusion in central nervous system and, more importantly, the pleiotropic actions triggered by their ability to bind multiple receptors (Longo and Massa, 2013 for review). In order to overcome such disadvantages of native neurotrophins, substantial efforts have been made to discover small molecules mimicking NGF actions with a better pharmacokinetics and receptor selectivity (Lee and Chao, 2001; Jang et al., 2007; Yamada et al., 2008; Scarpi et al., 2012). Most of these compounds act as robust Trk agonists that induce Trk signals even in the absence of NGF. Therefore, there still remains a concern about unexpected adverse on-target effects associated with highly activated Trk signaling. For example, early clinical trials that investigated the therapeutic efficacy of exogenously administered NGF had revealed unaccepted incidents of pain (Dyck et al., 1997; Eriksdotter Jonhagen et al., 1998; McArthur et al., 2000). Ironically, such clinical observations have largely provided a biological basis for the recent understandings that Trk-mediated NGF signaling play a key role in the peripheral sensitization process establishing chronic pain (see reviews by Bennett, 2001; Sah et al., 2003). Antagonism of NGF can prevent many of sensory abnormalities that develop in a number of animal models of inflammatory pain, further confirming the role of NGF in pain progression (Woolf et al., 1994; McMahon et al., 1995; Koltzenburg et al., 1999). In long-term clinical experiences in Japan, Neurotropin has never been reported to accentuate pain or other sensory abnormalities. This might be related to our present observations that Neurotropin, unlike other Trk agonists, demonstrated neuroprotection only when cells were lacking adequate trophic support.

4. Experimental procedure

4.1. Chemicals

All reagents were purchased from Sigma (MO, USA) unless stated otherwise. Neurotropin was provided from Nippon Zoki Pharmaceutical Co., Ltd. (Osaka, Japan). The analgesic activity of Neurotropin (expressed in Neurotropin unit, NU) is standardized by a behavioral testing in rodents loaded with the "stress alteration of rhythm in environmental temperature" (SART), a repeated cold stress by which hypersensitivity to a noxious stimulus is produced (Kita et al., 1979). Neurotropin does not contain detectable known proteins such as neurotrophins (HPLC). Neurotropin was diluted with saline (Otsuka, Tokushima, Japan) as a vehicle.

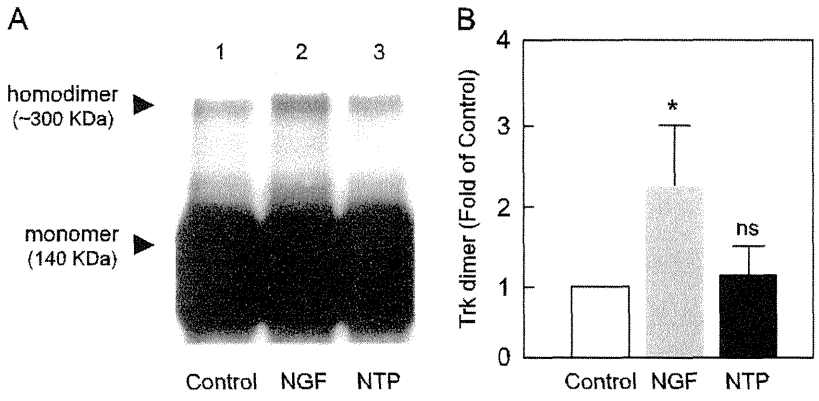

Fig. 5 – Effect of Neurotropin on dimerization of Trk in PCtrk cells. (A) PCtrk cells (5×10^5 cells) were incubated at 37 °C in serum-free DMEM with saline (Control; *lane* 1), NGF (50 ng/mL; *lane* 2), or Neurotropin (NTP; 20 mNU/mL; *lane* 3). Cell surface molecules were crosslinked by membrane-impermeable bifunctional crosslinker, BS3, at 4°C for 30 min. α-Trk immunoprecipitates of the cell lysates were subjected to SDS-7.5% PAGE for the detection of monomeric (approximately 140 kDa) and dimeric (approximately 300 kDa) forms of Trk by Western blot analysis. Each lane contained equal protein amount of lysates. Representative data was shown. (B) Intensity of Western blot for dimerized Trk derived from same protein amount of cell lysates was calculated by Image J as described in Section 4. Data represents the mean and SD of three independent experiments. *$P < 0.05$ vs. saline-treated controls; ns, not significant (Student *t*-test).

4.2. *Cell cultures*

PC12 cells overexpressing Trk (PCtrk cells) were constructed as described elsewhere (Mutoh et al., 2000). The cells were grown in DMEM (Invitrogen, CA, USA) supplemented with 2 mM L-glutamine, 5% horse serum and 5% fetal bovine serum (Biowhittaker, MD, USA) in polystyrene culture flasks or dishes (Becton Dickinson, NJ, USA) at 37 °C in an humidified chamber supplied with 5% CO_2. Expression of Trk in PCtrk cells is almost 10 fold greater than the parental PC12 cells cultured in normal DMEM. Viability of the cells was always more than 90% when assessed by staining dead cells with 0.4% Trypan Blue dye.

4.3. *Evaluations of cell differentiation*

Undifferentiated PCtrk cells (approx. 1000 cells per well) were allowed to adhere on 6-well plate surface, and stimulated with 2.5S NGF (Millipore, MA, USA) and/or Neurotropin for 18–24 h. For quantitative analysis, neurite length was measured under microscope by using Image J software (ver. 1.44; NIH, USA). Several typical fields containing at least 100 cells were randomly chosen to obtain total neurite length and the number of cell bodies. Total neurite length divided by the total numbers of cell bodies was defined as averaged neurite length (μm per cell). Three independent cultures were analyzed to calculate the mean and standard deviations (SD) of neurite length for each condition. In inhibition assay, K252a (500 nM; Biomol, PA, USA) was added simultaneously with NGF. For quantitative analysis, typical images of three independent cultures were captured under microscopy and analyzed as described above.

In addition to the morphological evaluation, expression of neurofilament, a major axonal constituent, was quantified. PCtrk cells (1×10^5) stimulated with or without NGF and/or Neurotropin were lysed and homogenized at 4 °C in SDS sample buffer (58.3 mM Tris–HCl, pH 6.8, 1.7% SDS, 5% glycerol, 3.3% 2-mercaptoethanol, 0.002% bromophenol blue). The lysate was boiled and stored at −80 °C for Western blot analysis as described below. Blot intensities by Western analysis against neurofilament M (NF-M) and β-actin were determined by Image J software to calculate relative NF-M expression per β-actin.

4.4. *Immunoprecipitation and immunoblotting*

PCtrk cells were stimulated with NGF following medium replacement by serum-free DMEM at least for 1 h. After NGF treatment, medium was removed and cells were immediately washed with ice-cold phosphate-buffered saline (PBS, pH 7.4), followed by solubilization in SDS sample buffer for whole-cell analysis, or in lysis buffer (20 mM HEPES, pH 7.2, 1% Nonidet P-40, 10% glycerol, 50 mM NaF, 1 mM phenylmethylsulfonyl fluoride, 1 mM Na3VO4, 10 μg/mL leupeptin). After centrifugation at 12,000 rpm for 2 min at 4 °C, the lysates were subjected to immunoprecipitation with an antibody against Trk (clone C-14; Santa Cruz Biotechnology, Santa Cruz, CA, USA, α-Trk) and protein A-Sepharose conjugate (Sigma, USA) at 4 °C overnight. After washing extensively, the precipitates were eluted from the Sepharose beads by boiling in SDS sample buffer for 5 min. The eluates were separated on SDS-5–20% PAGE (ePA-GEL; Atto Chemicals, Tokyo, Japan), and blotted onto PVDF membrane (Immobilon-P; Millipore, USA). The membranes were blocked for 1 h in Tris-buffered saline (TBS) containing 0.1% Tween 20 (TBS-T) with 3% nonfat milk. Incubations with the primary, as well as with the HRP-coupled secondary, antibodies were performed for 1 h at room temperature (RT) in TBS-T. Immunoreactive bands were visualized by an ECL detection system (ECL Plus; GE Healthcare, Buckinghamshire, UK). Antibodies used in this study were as follows: α-Trk (clone C-14), anti-phosphotyrosine monoclonal antibody (clone 4G10; Upstate, NY, USA; α–PY), anti-GM1 antisera (EMD Bioscience,

CA, USA; α–GM1), anti-neurofillament M antibody (NA1216; Affiniti Research, Devon, UK; α–NFM), and antibodies against ERK1/2, phospho-ERK1/2, Akt, and phospho-Akt (Cell Signaling Technologies, MA, USA) for primary antibodies; anti-rabbit IgG (AP132P; Chemicon International, CA, USA) and anti-mouse IgG (Amersham Bioscience, Buckinghamshire, UK) for secondary antibodies.

4.5. *Quantitative analysis for Trk autophosphorylation*

For quantitation of phosphorylated Trk, a double-antibody ELISA system was constructed. Briefly, a 96-well microplate (Immulon® 4 HBX; Thermo Electron, MA, USA) coated with 100 μL/well of α-Trk (1:1000 dilution) was blocked by 200 μL of TBS containing 3% nonfat milk. Lysates prepared from confluent cultures (1×10^5 cells) in 3-cm dishes were incubated in the wells for 2 h at RT. Each well contained an equal protein amount of lysate, determined by BCA protocol (Thermo Fisher Scientific, IL, USA). After washing with TBS-T, wells were incubated sequentially for 2 h with α–PY (1:1000 dilution, 100 μL) and anti-mouse IgG conjugated with HRP (1:2000 dilution, 100 μL). Bound enzyme activity was assessed by chromogenic substrate (TMB One; Promega, CA, USA) with optical density at 450 nm (OD 450) employing a microplate reader (Benchmark microplate reader; BioRad). In a separate experiment, OD 450 values in the assay were confirmed to be linearly related to the band intensities of Western blot analysis against phosphotyrosines in a-Trk immunoprecipitates.

4.6. *Trk homodimerization*

Trk dimerization was carried out as described by Fukumoto et al. (2000). Cells (5×10^6) were plated on 10-cm dishes and treated with NGF (50 ng/mL, 5 min) or Neurotropin (20 mNU/mL, 3 h) in serum-free DMEM. The medium was removed, and the cells were washed twice with ice-cold PBS, and cross-linked in a buffer (25 mM HEPES, pH 8.5, 120 mM NaCl, 6 mM KCl, 1 mM MgCl2, 10 mM EGTA) containing 1 mM bis (sulfosuccinimidyl) suberate (BS3) at 4 °C for 30 min. The reaction was terminated by adding 1 M Tris–HCl (pH 7.4) to a final concentration at 50 mM. Cells were then washed twice with TBS and lysed in a lysis buffer as described above. Cell lysates were subjected to SDS-7.5% PAGE, followed by Western blot analysis with α-Trk. Intensities of bands corresponding to the size of Trk monomer (140 kDa) and dimer (ca. 300 kDa) were quantified by Image J software. Each lane contained an equal amount of proteins.

4.7. *Statistics*

All data were analyzed after the completion of experiments by SAS system (version 8.2; SAS Institute, Japan). All significance tests used a level <0.05.

Conflict of interest

The affiliations of each author are noted in the citation appended to the list of authors. The authors have disclosed the following industry relationships: YF, TA, HI and KF are full-time employees of Nippon Zoki Pharmaceutical. Till 2008, APK had been a scientific advisor for Nippon Zoki Pharmaceutical. Other authors have no disclosure to report. All the experimental works included in this article was performed by YF with technical assistance by TF, CH, TI, and KM. TA, KF and HI did statistic analyses and quality assessment of the data. TM, AU, HI, KF and APK contributed to the article preparation.

Acknowledgments

We are grateful to Dr. Irwin J. Kopin (National Institutes of Health, USA) for helpful discussions. We also thank Ms. Chieko Nishikawa for her excellent technical assistance. This work was supported by the MUSC Foundation for Research Development (Charleston, SC, USA) to A.P.K., and by MEXT-Supported Program for the Strategic Research Foundation at Private Universities 2010–2014 and a grant-in-aid from the Ministry of Education, Culture, Sports, Science and Technology of Japan to T.M.

REFERENCES

Asakura, K., Ueda, A., Kawamura, N., Ueda, M., Mihara, T., Mutoh, T., 2009. Clioquinol inhibits NGF-induced Trk autophosphorylation and neurite outgrowth in PC12 cells. Brain Res. 1301, 110–115.

Bai, J., Nakamura, H., Kwon, Y.W., Hattori, I., Yamaguchi, Y., Kim, Y.C., Kondo, N., Oka, S., Ueda, S., Masutani, H., Yodoi, J., 2003. Critical roles of thioredoxin in nerve growth factor-mediated signal transduction and neurite outgrowth in PC12 cells. J. Neurosci. 23, 503–509.

Bennett, D.L., 2001. Neurotrophic factors: important regulators of nociceptive function. Neuroscientist 7, 13–17.

Chao, M.V., Rajagopal, R., Lee, F.S., 2006. Neurotrophin signalling in health and disease. Clin. Sci. 110, 167–173.

De Reuck, J., Decoo, D., Vanderdonckt, P., Dallenga, A., Ceusters, W., Kalala, J.P., De Meulemeester, K., Abdullah, J., Santens, P., Huybrechts, J., Spiers, R., De Bleecker, J., Tack, I., Tack, E., Vogels, C., Boon, P., 1994. A double-blind study of Neurotropin in patients with acute ischemic stroke. Acta Neurol. Scand. 89, 329–335.

Dyck, P.J., Peroutka, S., Rask, C., Burton, E., Baker, M.K., Lehman, K.A., Gillen, D.A., Hokanson, J.L., O'Brien, P.C., 1997. Intradermal recombinant human nerve growth factor induces pressure allodynia and lowered heat-pain threshold in humans. Neurology 48, 501–505.

Eriksdotter Jonhagen, M., Nordberg, A., Amberla, K., Backman, L., Ebendal, T., Meyerson, B., Olson, L., Seiger, Shigeta, M., Theodorsson, E., Viitanen, M., Winblad, B., Wahlund, L.O., 1998. Intracerebroventicular infusion of nerve growth factor in three patients with Alzheimer's disease. Dement. Geriatr. Cogn. Disord. 9, 246–257.

Farooqui, T., Franklin, T., Pearl, D.K., Yates, A.J., 1997. Ganglioside GM1 enhances induction by nerve growth factor of a putative dimer of TrkA. J. Neurochem. 68, 2348–2355.

Fukuda, Y., Berry, T.L., Nelson, M., Hunter, C.L., Fukuhara, K., Imai, H., Ito, S., Granholm-Bentley, A.-C., Kaplan, A.P., Mutoh, T., 2010. Stimulated neuronal expression of brain-derived neurotrophic factor by Neurotropin. Mol. Cell. Neurosci. 45, 226–233.

Fukumoto, S., Mutoh, T., Hasegawa, T., Miyazaki, H., Okada, M., Goto, G., Furukawa, K., Urano, T., Furukawa, K., 2000. GD3 synthase gene expression in PC12 cells results in the continuous activation of TrkA and ERK1/2 and enhanced proliferation. J. Biol. Chem. 275, 5832–5838.

Greene, L.A., Tischler, A.S., 1976. Establishment of a noradrenergic clonal line of rat adrenal pheochromocytoma cells which respond to nerve growth factor. Proc. Natl. Acad. Sci. U.S.A. 73, 2424–2428.

Hakomori, S.-I., 2000. Cell adhesion/recognition and signal transduction through glycosphingolipid microdomain. Glycoconj. J. 17, 143–151.

Hatanaka, H., 1981. Nerve growth factor-mediated stimulation of tyrosine hydroxylase activity in a clonal rat pheochromocytoma cell line. Brain Res. 222, 225–233.

Hemstead, B.L., Rabin, S.J., Kaplan, L., Reid, S., Parada, L.F., Kaplan, D.R., 1992. Overexpression of the trk tyrosine kinase rapidly accelerates nerve growth factor-induced differentiation. Neuron 9, 883–896.

Hoshino, Y., Nakamura, T., Sato, A., Mishima, M., Yodoi, J., Nakamura, H., 2007. Neurotropin demonstrates cytoprotective effects in lung cells through the induction of thioredoxin-1. Am. J. Respir. Cell. Mol. Biol. 37, 438–446.

Huang, E.J., Reichardt, L.F., 2003. Trk receptors: roles in neuronal signal transduction. Annu. Rev. Biochem. 72, 609–642.

Indo, Y., Tsuruta, M., Hayashida, Y., Karim, M.A., Ohta, K., Kawano, T., Mitsubuchi, H., Tonoki, H., Awaya, Y., Matsuda, I., 1996. Mutations in the TRKA/NGF receptor gene in patients with congenital insensitivity to pain with anhidrosis. Nat. Genet. 13, 485–488.

Jang, S.-W., Okada, M., Sayeed, I., Xiao, G., Stein, D., Jin, P., Ye, K., 2007. Gambogic amide, a selective agonist for TrkA receptor that possesses robust neurotrophic activity, prevents neuronal cell death. Proc. Natl. Acad. Sci. U.S.A. 104, 16329–16334.

Jing, S., Tapley, P., Barbacid, M., 1992. Nerve growth factor mediates signal transduction through trk homodimer receptors. Neuron 9, 1067–1079.

Kaplan, D.R., Martin-Zenca, D., Parada, J.F., 1991a. Tyrosine phosphorylation and tyrosine kinase activity of the trk proto-oncogene product induced by NGF. Nature 350, 158–160.

Kaplan, D.R., Hemsprcad, B.L., Martin-Zenca, D., Chao, M.V., Parada, L.F., 1991b. The Trk proto-oncogene product: a signal transducing receptor for nerve growth factor. Science 252, 554–558.

Kawashiri, T., Egashira, N., Itoh, Y., Shimazoe, T., Ikegami, Y., Yano, T., Yoshimura, M., Oishi, R., 2009. Neurotropin reverses paclitaxel-induced neuropathy without affecting anti-tumour efficacy. Eur. J. Cancer 45, 154–163.

Kawashiri, T., Egashira, E., Watanabe, H., Ikegami, Y., Hirakawa, S., Mihara, Y., Yano, T., Ikesue, H., Oishi, R., 2011. Prevention of oxaliplatin-induced mechanical allodynia and neurodegeneration by Neurotropin in the rat model. Eur. J. Pain 15, 344–350.

Kimura, H., Nakamura, S., Okamoto, K., Toyama, I., Watanabe, M., Ikeuchi, K., 1987. A pilot study for clinical application of Neurotropin to senile patients with dementia. Jpn. Pharmacol. Ther. 15, 407–423 (in Japanese).

Kita, T., Hata, T., Iida, J., Yoneda, R., Ishida, S., 1979. Decrease in pain threshold in SART stressed mice. Jpn. J. Pharmacol. 29, 479–482.

Koltzenburg, M., Bennett, D.L., Shelton, D.L., McMahon, S.B., 1999. Neutralization of endogenous NGF prevents the sensitization of nociceptors supplying inflamed skin. Eur. J. Neurosci. 11, 1698–1704.

Lee, F.S., Chao, M.V., 2001. Activation of Trk neurotrophin receptors in the absence of neurotrophins. Proc. Natl. Acad. Sci. U.S.A. 98, 3555–3560.

Limpert, A.S., Karlo, J.C., Landreth, G.E., 2007. Nerve growth factor stimulates the concentration of TrkA within lipid rafts and extracellular signal-regulated kinase activation through c-Cbl-associated protein. Mol. Cell. Biol. 27, 5686–5698.

Longo, F.M., Massa, S.M., 2013. Small-molecule modulation of neurotrophin receptors: a strategy for the treatment of neurological disease. Nat. Rev. 12, 507–525.

McArthur, J.C., Yiannoutsos, C., Simpson, D.M., Adornato, B.T., Singer, E.J., Hollander, H., Marra, C., Rubin, M., Cohen, B.A., Tucker, T., Navia, B.A., Schifitto, G., Katzenstein, D., Rask, C., Zaborski, L., Smith, M.E., Shriver, S., Millar, L., Clifford, D.B., Karalnik, I.J., 2000. A phase II trial of nerve growth factor for sensory neuropathy associated with HIV infection. AIDS Clinical Trials Group Team 291. Neurology 54, 1080–1088.

McMahon, S.B., Bennett, D.L., Priestley, J.V., Shelton, D.L., 1995. The biological effects of endogenous NGF in adult sensory neurons revealed by a trk-IgG fusion molecule. Nat. Med 1, 774–780.

Morita, S., Takeoka, Y., Imai, H., Yamamoto, H., Suchiro, S., Ueda, S., Katoh, S., 1998. Differential action of nerve growth factor, cyclic AMP and Neurotropin on PC12h cells. Cell Struct. Funct. 13, 227–234.

Mutoh, T., Tokuda, A., Miyadai, T., Hamagichi, M., Fujiki, N., 1995. Ganglioside GM1 binds to the Trk protein and regulates receptor function. Proc. Natl. Acad. Sci. U.S.A. 92, 5087–5091.

Mutoh, T., Tokuda, A., Inokuchi, J., Kuriyama, M., 1998. Glucosylceramide synthase inhibitor inhibits the action of nerve growth factor in PC12 cells. J. Biol. Chem. 273, 26001–26007.

Mutoh, T., Hamano, T., Tokuda, A., Kuriyama, M., 2000. Unglycosylated Trk protein does not co-localize nor associate with ganglioside GM1 in stable clone of PC12 cells overexpressing Trk (PCtrk cells). Glycoconj. J. 17, 233–237.

Mutoh, T., Tachi, M., Yano, S., Mihara, T., Yamamoto, H., 2005. Impairment of Trk-neurotrophin receptor by the serum of a patient with subacute sensory neuropathy. Arch. Neurol. 62, 1612–1615.

Patapoutian, A., Reichardt, L.F., 2001. Trk receptors: mediators of neurotrophin action. Curr. Opin. Neurobiol. 11, 272–280.

Pike, L.J., 2003. Lipid rafts: bringing order to chaos. J. Lipid Res. 44, 655–667.

Rabin, S.J., Mocchetti, I., 1995. GM1 ganglioside activates the high-affinity nerve growth factor receptor trkA. J. Neurochem. 65, 347–354.

Scarpi, D., Cirelli, D., Matrone, C., Castronovo, G., Rosini, P., Occhiato, E.G., Romano, F., Bartali, L., Clemente, A.M., Bottegoni, G., Cavalli, A., De Chiara, G., Bonini, P., Calissano, P., Palamara, A.T., Garaci, E., Torcia, M.G., Guarna, A., Cozzolino, F., 2012. Low molecular weight, non-peptidic agonists of TrkA receptor with NGF-mimetic activity. Cell Death Dis 3, e339.

Sah, D.W.Y., Ossipov, M.H., Porreca, F., 2003. Neurotrophic factors as novel therapeutics for neuropathic pain. Nat. Rev. Drug Discovery 2, 460–472.

Sobue, I., Tashiro, K., Hanakago, R., Ando, K., Yamada, T., Iida, M., Nishitani, H., Saida, K., Konishi, T., Takayanagi, T., Doi, R., Ohmura, I., Hirose, N., Takase, Y., Iwashita, H., Koike, F., Igata, A., Tanabe, H., Matsumoto, A., Ogawa, N., Hirai, S., 1992. Clinical evaluation of Neurotropin injections on dysesthesia of SMON (subacute myelo-optico-neuropathy). A multi-institutional double-blind comparative study. Rinsyo Iyaku 8, 833–847 (in Japanese).

Sofroniew, M.V., Howe, C.L., Mobley, W.C., 2001. Nerve growth factor signaling, neuroprotection, and neural repair. Ann. Rev. Neurosci. 24, 1217–1281.

Woolf, C.J., Safieh-Garabedian, B., Ma, Q.P., Crilly, P., Winter, J., 1994. Nerve growth factor contributes to generation of inflammatory sensory hypersensitivity. Neuroscience 62, 327–331.

Yamada, M.K., Konishi, Y., Kakinoki, B., Ikegami, K., Setou, M., 2008. Enhancement of Trk signaling pathways by the cholestane amide conjugate MCC-257. J. Pharmacol. Sci. 108, 131–134.

Zhang, R.X., Lu, Z.H., Wan, D.S., Wu, X.J., Ding, P.R., Kong, L.H., Pan, Z.Z., Chen, G., 2012. Neuroprotective effect of neurotropin on chronic oxaliplatin-induced neurotoxicity in stage II and stage III colorectal cancer patients: results from a prospective, randomized, single-centre, pilot clinical trial. Int. J. Colorectal Dis. 27, 1645–1650.

Toxicology 331 (2015) 112–118

Contents lists available at ScienceDirect

Toxicology

journal homepage: www.elsevier.com/locate/toxicol

Histone deacetylase inhibitor attenuates neurotoxicity of clioquinol in PC12 cells

Takao Fukui, Kunihiko Asakura *, Chika Hikichi, Tomomasa Ishikawa, Rie Murai, Seiko Hirota, Ken-ichiro Murate, Madoko Kizawa, Akihiro Ueda, Shinji Ito, Tatsuro Mutoh

Department of Neurology, Fujita Health University School of Medicine, 1-98 Kutsukake-cho, Toyoake, Aichi 470-1192, Japan

ARTICLE INFO

Article history:
Received 5 December 2014
Received in revised form 19 January 2015
Accepted 20 January 2015
Available online 7 March 2015

Keywords:
Clioquinol
Deacetylation of histones
Histone deacetylase inhibitor
Subacute myeloopticoneuropathy

ABSTRACT

Clioquinol is considered to be a causative agent of subacute myelo-optico neuropathy (SMON), although the pathogenesis of SMON is yet to be elucidated. We have previously shown that clioquinol inhibits nerve growth factor (NGF)-induced Trk autophosphorylation in PC12 cells transformed with human Trk cDNA. To explore the further mechanism of neuronal damage by clioquinol, we evaluated the acetylation status of histones in PC12 cells. Clioquinol reduced the level of histone acetylation, and the histone deacetylase (HDAC) inhibitor Trichostatin A upregulated acetylated histones and prevented the neuronal cell damage caused by clioquinol. In addition, treatment with HDAC inhibitor decreased neurite retraction and restored the inhibition of NGF-induced Trk autophosphorylation by clioquinol. Thus, clioquinol induced neuronal cell death via deacetylation of histones, and HDAC inhibitor alleviates the neurotoxicity of clioquinol. Clioquinol is now used as a potential medicine for malignancies and neurodegenerative diseases. Therefore, HDAC inhibitors can be used as a candidate medicine for the prevention of its side effects on neuronal cells.

1. Introduction

Subacute myelo-optico neuropathy (SMON) mainly occurred during 1950–1960s in Japan (Tsubaki et al., 1971; Sobue, 1979; Shiraki, 1979) and was characterized by subacute onset of sensory and motor disturbances in the lower extremities with visual impairment (Nakae et al., 1973; Tsubaki et al., 1971). Neuropathological study demonstrated distal dominant axonopathy of the spinal long tracts and optic tracts (Tateishi, 2000). Clioquinol (5-chloro-7-iodo-8-hydroxyquinoline), which had been used as an antibiotic for treating diarrhea and skin infection, has been considered to be a causative agent for SMON. More than 10,000 patients in Japan were affected by SMON before the discontinuation of therapeutic use in clinical practices in Japan. After the ban of the sale of clioquinol in September 1970, there was a drastic disappearance of new cases of SMON though nearly 3000 patients still suffer from its sequelae in 2002 (Konagaya et al., 2004). Even after 40 years of the outbreak of SMON in Japan, the mechanism of neuronal cell damage by clioquinol is yet to be elucidated. Recently clioquinol has been shed the light on as a possible treatment for malignancies (Chen et al., 2007) and neurodegenerative diseases including Alzheimer's disease, Parkinson's disease, and Huntington's disease (Cherny et al., 2001; Ritchie et al., 2003; Kaur et al., 2003; Nguyen et al., 2005). Given the potential reintroduction of oral clioquinol medication for these new indications, a clear understanding of clioquinol neurotoxicity is essential to fully appreciate the potential side effects of this drug. To explore the mechanism of neurotoxicity of clioquinol, we previously showed that clioquinol inhibits nerve growth factor (NGF)-induced Trk receptor autophosphorylation in PC12 cells transformed with human *trk* cDNA (the PCtrk neuronal cell line) (Asakura et al., 2009). There are some other potential mechanisms regarding clioquinol neurotoxicity. In SH-SY5Y and IMR-32 neuroblastoma cells, clioquinol induced neurotoxicity mediated by DNA double-strand breaks (DSBs) and subsequent activation of ATM/p53 signaling pathway (Katsuyama et al., 2012). Other study has indicated that clioquinol inhibited the activity of SOD-1 and therefore enhances reactive oxygen species in SH-SY5Y cells (Kawamura et al., 2014).

Acetylation of histones is closely related to the cell fate decisions between survival and death. Histone deacetylases (HDACs) are enzymes that deacetylate lysine residues from

* Corresponding author. Tel.: +81 562 93 9295; fax: +81 562 93 1856.
E-mail address: kasakura@fujita-hu.ac.jp (K. Asakura).

http://dx.doi.org/10.1016/j.tox.2015.01.013
0300-483X/

histones as well as from several other nuclear, cytoplasmic and mitochondrial non-histone proteins. In mammals, 18HDACs have been phylogenetically classified into four classes. Classes I, II, and IV are usually referred as classical HDACs and are categorized based on their homology to yeast proteins, Rpd3 and Hda1 (Ververis and Karagiannis, 2011). Class I, II, and IV HDACs are zinc-dependent enzymes (Gräff and Tsai, 2013). Class I HDAC includes the constitutively expressed HDACs 1, 2, 3 and 8 (Walkinshaw et al., 2008). Class II is subdivided into classes IIa (HDAC4, 5, 7, and 9) and IIb (HDAC6 and 10). Enzymes from class IIa are able to shuttle between the cytosol and the nucleus, and show a weaker deacetylase activity (Lahm et al., 2007). Class IIb is mostly found in the cytosol with a preference for non-histone proteins (Boyault et al., 2007), and HDAC11 is the sole member of class IV. Class III, called sirtuins, are NAD^+ (nicotinamide adenine dinucleotide)-dependent enzymes with distinct structural features (Haberland et al., 2009).

Therefore, HDAC inhibitors are capable of inducing widespread alterations in cellular function and protein expression through posttranslational modification of histones, transcriptional factors, and heat shock shaperones (Lu et al., 2011; Fischer et al., 2010; Minucci and Pelicci, 2006). In this study, we further confirm the underlying mechanism of clioquinol neurotoxicity via histone deacetylation. Intriguingly, HDAC inhibitor attenuates its neurotoxicity in a neuronal cell line.

2. Materials and methods

2.1. Cell culture

PC12 cells transformed with human Trk cDNA (PCtrk cells) were cultured in Dulbecco's modified Eagle's medium (DMEM) supplemented with 10% horse serum, 5% fetal bovine serum, 100 U/ml penicillin, and 100 mg/ml streptomycin (Mutoh et al., 2000). Clioquinol was purchased from Sigma (St. Louis, MO, USA) and was dissolved in 100% DMSO at a final concentration of 10 mM as a stock solution. The stock solution was further diluted for various experiments. To exclude the cellular toxicity of DMSO to PCtrk cells, the vehicle containing equivalent amount of DMSO was previously examined (Asakura et al., 2009). We confirmed that cells were not affected by DMSO up to 0.2% concentration (Asakura et al., 2009).

To examine the effect of clioquinol on differentiated neuronal cells, PCtrk cells were treated with 50 ng/ml of NGF in serum-free medium overnight, then the neurite-extended cells were cultured with 50 ng/ml NGF and 1 μM clioquinol for up to 15 h. The cells were observed under phase contrast microscope. NGF-stimulated PCtrk cells were also cultured with 0.1 μM Trichostatin A (TSA) (Sigma), which inhibits class I and II histone deacetylase (HDAC), 2 h prior to the addition of 1 μM clioquinol.

2.2. Western blotting

Extracted proteins from PCtrk cells were separated by sodium dodecyl sulfate-polyacrylamide electrophoresis (SDS-PAGE) under reducing conditions, and then transferred to polyvinylidene difluoride (PVDF) membranes by electroblotting. The membranes were incubated with rabbit anti-histone H3 monoclonal antibody (Cell Signaling Technology, Danvers, MA, USA) or rabbit anti-acetyl-histone H3 (Lys9) monoclonal antibody (Cell Signaling Technology) overnight at 4 °C after blocking with Tris-buffered saline containing 5% non-fat dry milk and 0.05% Tween 20 for 1 h at room temperature. Bound antibody was then detected with biotinylated anti-mouse or anti-rabbit IgG and horseradish peroxidase-conjugated streptavidin (both from Jackson ImmunoResearch Laboratories Inc., West Gove, PA, USA) using the enhanced chemiluminescence (ECL) system (Amersham Pharmacia Biotech, Piscataway, NJ, USA). We also examined the acetylated levels of microtubule, α-tubulin using anti-α-tubulin (rabbit monoclonal,

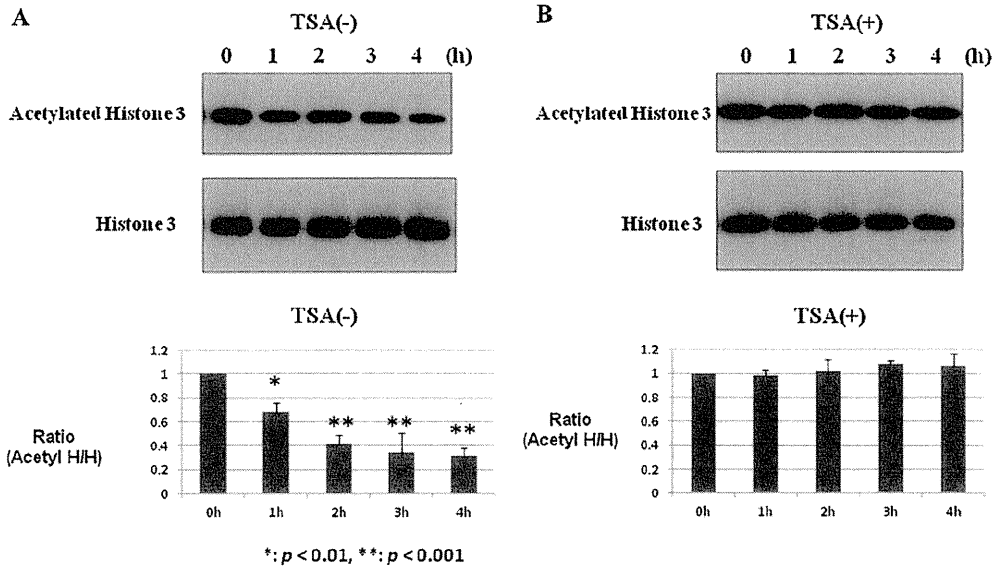

Fig. 1. Clioquinol reduces the level of acetylated histone, whereas the HDAC inhibitor TSA, increases the level of acetylated histone.
(A) The proteins extracted from the cells cultured with 1 μM clioquinol for 0–4 h were separated by SDS-PAGE. Acetylated histone 3 and histone 3 were detected by western blotting. The experiments at each time point were performed in triplicate. Bars and error bars represent means ± SD. Statistical analysis by Mann–Whitney *U* test was performed, *: $p < 0.01$, **: $p < 0.001$.
(B) NGF-stimulated cells were treated with 0.1 μM TSA 2 h prior incubation, then the cells were cultured with 1 μM clioquinol and 0.1 μM TSA. Acetylated histone 3 and histone 3 were detected by western blotting. At each time point, the level of acetylated histone 3 was adjusted with histone 3, respectively, and was compared as a ratio.

Cell Signaling Technology) and anti-acetyl-α-tubulin (rabbit monoclonal, Cell Signaling Technology) antibodies.

2.3. Neurite retraction assay and cell survival assay

We examined the effect of clioquinol on NGF-stimulated PCtrk cells. To investigate the morphological effects on differentiated cells, the cells were seeded onto 6-well culture plates and the cells were cultured with 50 ng/ml of NGF in serum-free medium overnight. Overnight NGF stimulation induced morphological differentiation in 95–98% of the cells. Phase contrast micrographs were taken from typical areas of these cultures at 0, 1, 2, 3, and 4 h after the addition of 1 μM clioquinol. To examine the effect of HDAC inhibitor 0.1 μM TSA was added 2 h prior to the addition of clioquinol. Morphological changes were also quantitated at 0, 1, 2, 3, and 4 h after the addition of 1 μM clioquinol. The length of neurites of attached cells was measured by image processing and analysis software, Image J (NIH). Branched or unbranched neurites were traced and measured from the cell body to the tips of neurites. Each 50 cells from three independent wells were evaluated. Statistical analysis was performed by Mann–Whitney *U* test.

Furthermore, PCtrk cells were seeded onto 24-well plates and were stimulated with 50 ng/ml of NGF in serum-free medium overnight, then the differentiated neurite-extended cells were cultured with 50 ng/ml of NGF and 1 μM clioquinol overnight (15 h). HDAC inhibitor, 0.1 μM TSA, was also added 2 h prior to the addition of clioquinol. To detect the cell survival, the cells were incubated with trypan blue (Sigma). Under phase contrast microscope, the number of viable (unstained) and dead (stained) cells was counted. Each experiment was performed in triplicate, and statistical analysis was performed by Mann–Whitney *U* test.

2.4. Trk autophosphorylation

Cells were preincubated with serum-free medium for 1 h at 37 °C, and the cells were incubated in the presence of 1 μM clioquinol for 1 h. To examine the effect of HDAC inhibitor, cells were preincubated with serum-free medium for 1 h at 37 °C, and the cells were incubated in the presence of 0.1 μM TSA for 2 h prior to the addition of 1 μM clioquinol. Then, the cells were stimulated with 50 ng/ml of NGF for 5 min to examine the effect of clioquinol on NGF-induced Trk autophosphorylation. After stimulation, the cells were collected with chilled phosphate-buffered saline and lysed with lysis buffer (20 nM HEPES, pH7.2/1% Nonidet P-40/10% (vol./vol.) glycerol/50 mM NaF/1 mM phenylmethylsulfonyl fluoride (PMSF)/1 mM Na3VO4/10 μg of leupeptin per ml). The cell-free lysates were normalized for protein (1 mg/ml) and immunoprecipitated with anti-Trk antibody (α-Trk; Santa Cruz Biotechnology Inc., Dallas, TX, USA). Trk-immunoprecipitates were separated by SDS-PAGE under reducing conditions on 7–14% gradient acrylamide gels, which was followed by blotting on PVDF membranes. Tyrosine phosphorylation of the Trk protein was detected with an anti-phosphotyrosine antibody (α-PY; Upstate Biotechnology Inc., Waltham, MA, USA) and Trk was detected with α-Trk. The positive bands were detected with horseradish peroxidase-conjugated secondary antibodies using enhanced chemiluminescence (Amersham Pharmacia Biotech, Piscataway, NJ, USA) (Mutoh et al., 1995; Asakura et al., 2009). All experiments were performed in triplicate and statistical analysis by Mann–Whitney *U* test was done. Phosphorylated Trk at each condition was adjusted with total Trk protein, respectively, and was compared as a ratio. The ratio was calculated when compared to without NGF stimulation.

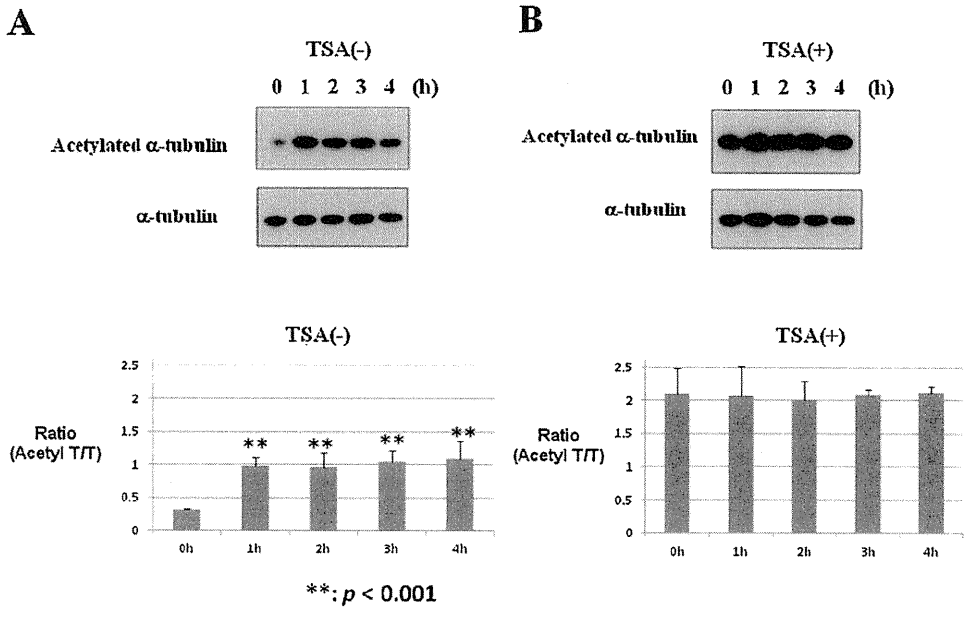

Fig. 2. Clioquinol increases acetylation of α-tubulin and TSA retained high levels of acetylated α-tubulin.
(A) The proteins extracted from the cells cultured with 1 μM clioquinol for 0–4 h were separated by SDS-PAGE. Acetylated α-tubulin and α-tubulin were detected by western blotting. The experiments at each time point were performed in triplicate. The bands were semi-quantitated by image analysis. Bars and error bars represent means ± SD. **: $p < 0.001$. The values are given as a ratio of acetylated α-tubulin/α-tubulin.
(B) NGF-stimulated cells were treated with 0.1 μM TSA 2 h prior incubation, then the cells were cultured with 1 μM clioquinol and 0.1 μM TSA. Acetylated α-tubulin and α-tubulin were detected by western blotting. At each time point, the values are given as a ratio of acetylated α-tubulin/α-tubulin.

3. Results

3.1. Clioquinol reduces the level of acetylated histone and HDAC inhibitor, TSA, increases the level of acetylated histone

We previously examined the molecular mechanisms for the cytotoxicity of clioquinol to NGF-stimulated PCtrk cells and clioquinol induced cell death in a concentration dependent manner (Asakura et al., 2009). 1 μM of clioquinol drastically increased cell death in NGF-stimulated cells at 24 h (Asakura et al., 2009). We, therefore, employed a concentration of 1 μM clioquinol in the following experiments.

The proteins extracted from the cells cultured with 1 μM of clioquinol for 0–4 h were applied for SDS-PAGE. Acetylated histone 3 and histone 3 were detected by western blotting. As shown in Fig. 1A, acetylated histone 3 was gradually decreased over time, whereas the expression of histone 3 was not changed. Semi-quantitative analysis showed that the ratio of acetylated histone 3/histone 3 was decreased down to 0.6–0.7 in 1 h when compared with initial state and the ratio was gradually decreased further with time (Fig. 1B).

PCtrk cells treated with NGF overnight were pre-treated with 0.1 μM of TSA for 1 h. Then, the cells were cultured with 1 μM of clioquinol and 0.1 μM of TSA for 0 to 4 h. In the presence of TSA, the amount of acetylated histone 3 expression was unchanged by clioquinol (Fig. 1A) and semi-quantitative analysis showed that the ratio of acetylated histone 3/histone 3 was not changed (Fig. 1B).

Besides histone 3, we also examined the levels of acetylated α-tubulin. Clioquinol increased the level of acetylated α-tubulin when compared to initial state. The ratio of acetylated α-tubulin/α-tubulin was not changed from 1 to 4 h (Fig. 2A). Pretreatment with TSA prominently increased acetylation of α-tubulin (Fig. 2B). High levels of acetylated α-tubulin were retained and the ratio of acetylated α-tubulin/α-tubulin was not changed from 0 to 4 h (Fig. 2B).

3.2. HDAC inhibitor reduces morphological changes (neurite retraction) and neuronal cell death following clioquinol treatment

NGF-stimulated cells were cultured with 1 μM clioquinol and were observed under phase contrast microscope for 0 to 4 h. NGF-stimulated cells extended the neurite, whereas clioquinol induced neurite retraction as previously reported (Asakura et al., 2009). 1 μM of clioquinol induced neurite retraction and some of the cells were rounded up and detached from the culture dishes (Fig. 3A). After 4 h incubation with clioquinol, 30–40% of total length of neurites was retracted. When 0.1 μM TSA was added 2 h prior to the clioquinol addition to the cells, the extended neurite were significantly less retracted (Fig. 3B and C).

NGF-stimulated cells were cultured either with 1 μM clioquinol or 1 μM clioquinol and 0.1 μM TSA. As shown in Fig. 4, 40–50% of the cells were dead after overnight incubation with clioquinol. In contrast, the presence of TSA in culture medium significantly reduced clioquinol-induced cell death.

3.3. HDAC inhibitor blocks the inhibition of NGF-induced Trk receptor autophosphorylation by clioquinol

A mature form of Trk and its precursor form were recognized as 140 kDa and 110 kDa, respectively. The immunoblot analysis with α-PY revealed a single band at 140 kDa corresponding to phosphorylated Trk (Fig. 5A). To examine the effects of clioquinol on NGF-induced Trk autophosphorylation, PCtrk cells were incubated in the presence of 1 μM clioquinol for 1 h followed by

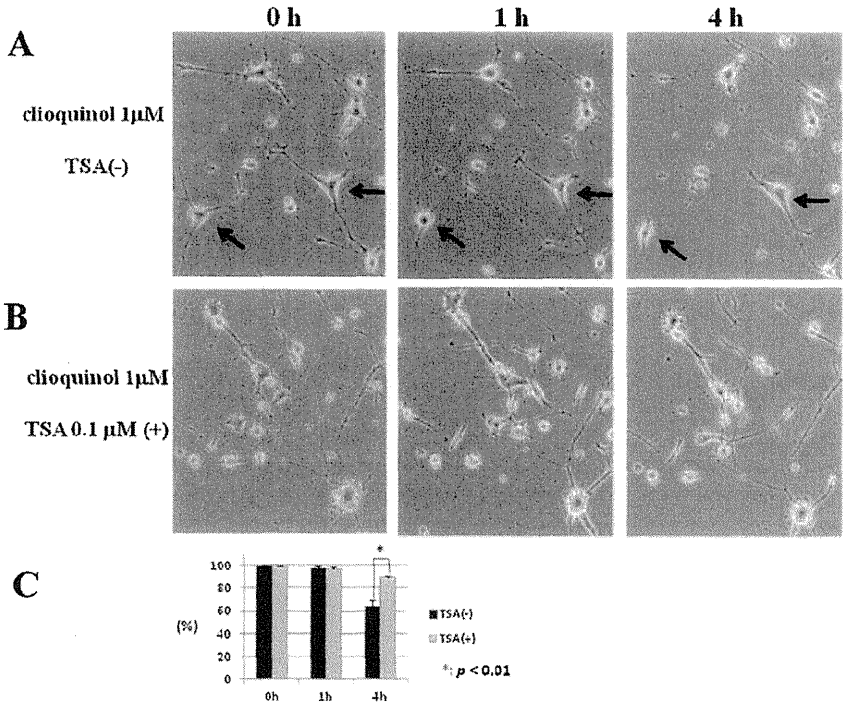

Fig. 3. Morphological effects of clioquinol and TSA on NGF-stimulated differentiated cells.
(A) NGF-stimulated cells were cultured with 1 μM of clioquinol and were observed under phase contrast microscope for 0–4 h. Arrows indicate prominent neurite-retracted cells. (B) NGF-stimulated cells were cultured with 0.1 μM TSA for 2 h prior to the clioquinol addition. Then, the cells were cultured with 1 μM clioquinol and 0.1 μM TSA. (C) Quantitative analysis of neurite. Phase contrast micrographs were taken from typical areas of these cultures. The length of neurites of attached cells was measured by image processing and analysis software, Image J (NIH). Each 50 cells from three independent wells were evaluated. Bars and error bars represent means ± SD. *: $p < 0.01$.

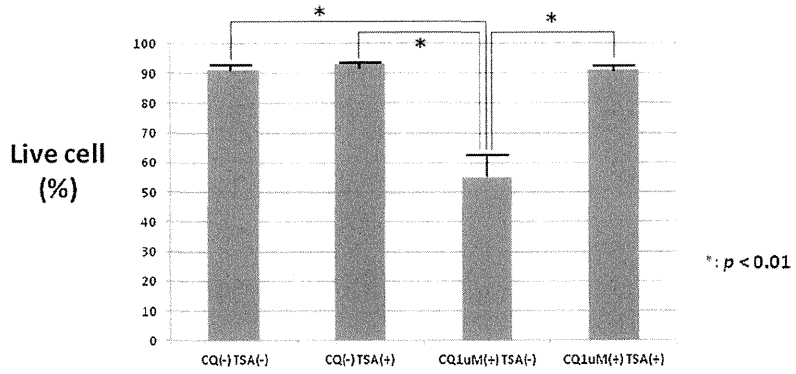

Fig. 4. Cell viability assay by trypan blue staining. NGF-stimulated cells were cultured with 1 μM clioquinol or 1 μM clioquinol + 0.1 μM TSA overnight. Live and dead cells were counted by trypan blue staining. Each experiment was performed in triplicate. Bars and error bars represent means ± SD. Note the TSA significantly blocks the toxicity of clioquinol. *: $p < 0.01$. (For interpretation of the references to color in this Fig. legend, the reader is referred to the web version of this article.)

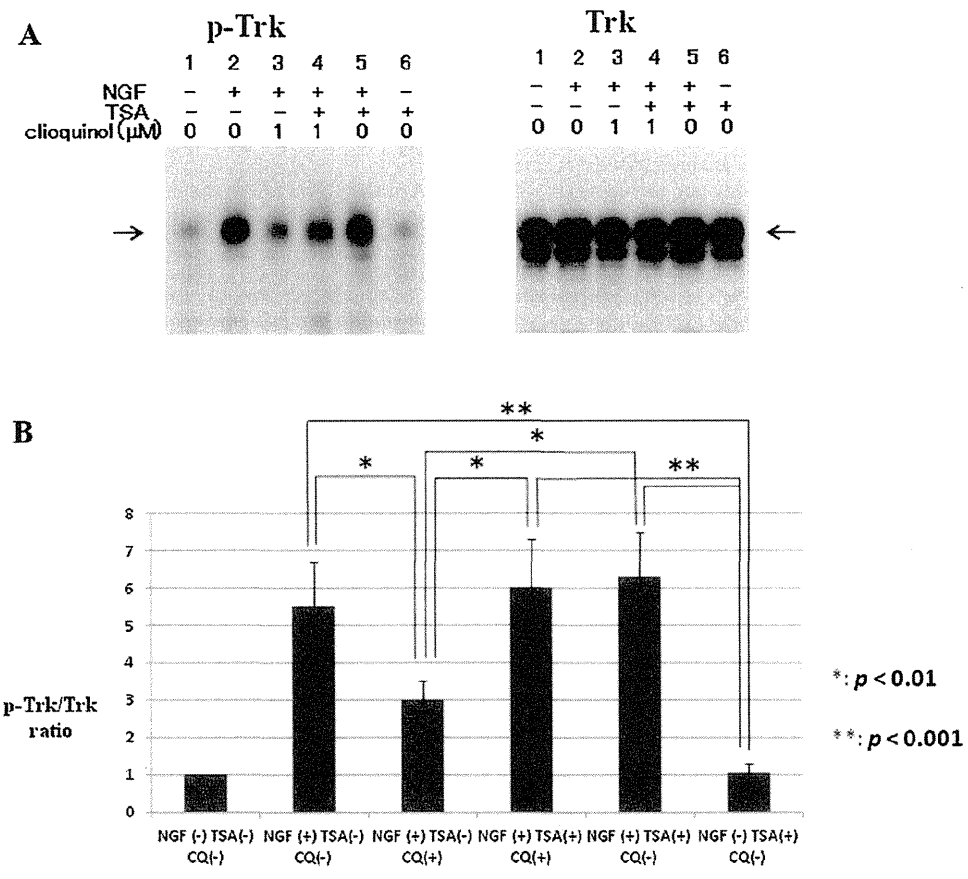

Fig. 5. Trk autophosphorylation by NGF.
(A) PCtrk cells were incubated with 1 μM clioquinol for 1 h, then, the cells were stimulated with 50 ng/ml of NGF for 5 min. Cell-free lysates were immunoprecipitated with α-Trk. Trk immunoprecipitates were subjected to SDS-PAGE and were immunoblotted either with anti-phosphotyrosine antibody (α-PY) or α-Trk. All experiments were performed in triplicate and Fig. 4A showed representative immunoblotting results. p-Trk indicates tyrosine phosphorylated Trk.
(B) Phosphorylated Trk at each condition was adjusted with total Trk protein, respectively, and was compared as a ratio. Bars and error bars represent means ± SD. *: $p < 0.01$.

the stimulation with NGF for 5 min. The cells were lysed with lysis buffer. To examine the effect of HDAC inhibitor, cells were preincubated with 0.1 μM TSA for 2 h, and the cells were incubated in the presence of 1 μM clioquinol for another 1 h. Then, the cell-free lysates were immunoprecipitated with α-Trk and the immunoprecipitates were immunoblotted with α-PY. As shown in the Fig. 5, the inhibition of NGF-induced Trk autophosphorylation by clioquinol was clearly observed. Semi-quantitative analysis showed that TSA significantly rescues the inhibition of NGF-induced Trk autophosphorylation by clioquinol.